GEOLOGIJA 67/2, 285-300, Ljubljana 2024

https://doi.org/10.5474/geologija.2024.014

Mineralogy, geochemistry and genesis of low-grade manganese ores of Anujurhi area, Eastern Ghats, India

Mineralogija, geokemija in geneza revnih manganovih rud z območja Anujurhi, Vzhodni Gati, Indija

Sujata PATTNAIK[1]* & Satrughan MAJHI[2]

[1]Geological Survey of India, Eastern Region, Bhu-Bijnan bhawan, DK-6, Karunamayee, Sector-2, Salt Lake, Kolkata-700091;
*corresponding author: suji.pinky@gmail.com
[2]Geological Survey of India, State Unit: Odisha, Unit-8, Nayapalli, Bhubaneswar-751012

Prejeto / Received 18. 3. 2024; Sprejeto / Accepted 12. 11. 2024; Objavljeno na spletu / Published online 16. 12. 2024

Key words: Eastern Ghats Mobile Belt (EGMB), Anujurhi, manganese ore, supergene enrichment
Ključne besede: Vzhodni Gati, Anujurhi, manganova ruda, supergena obogatitev

Abstract

The Anujurhi manganese ores occur in the high-grade gneisses of the Precambrian Eastern Ghats Supergroup in Odisha, India. They are characterized by conformable lenses containing minerals such as cryptomelane, romanechite, pyrolusite, todorokite, and pyrophanite, along with other opaque minerals like graphite, goethite and ilmenite. The gangue minerals associated with these ores include quartz, feldspar, garnet, kaolinite, apatite, sillimanite, zircon, biotite, alunite, and gorceixite. The primary elements present in the ore, Si, Mn, Fe, and Al, average at 16.20 %, 15.06 %, 11.94 %, and 6.6 % respectively. Additionally, trace amounts of P, K, Ti, Mg, Ca, and Na were detected. The average Fe/Mn ratio of 0.81 and the Si *versus* Al plot of the Anujurhi manganese ores suggest a hydrogenous-hydrothermal mixed source for the ferromanganese sediments. The characteristics of the manganese ore bands, absence of carbonate facies of ore, and geochemical association of Mn-Ba together with Na/Mg ratios and CaO-Na_2O-MgO ternary plot of the manganese ores strongly indicate that the mineralization is a metamorphosed shallow marine-lacustrine deposit. Following deposition and diagenesis, the manganese minerals underwent at least two phases of Ultra High Temperature (UHT) and granulite facies metamorphism along with the host rocks. Tectonic uplift, erosion, extended exposure to atmospheric oxygen and percolation of meteoric water led to the supergene alteration and remobilization of the primary manganese minerals in a colloidal state, followed by epigenetic replacement along the structural weak planes of the granulite facies rocks, resulting in the formation of the current deposits. This is evidenced by the observed secondary replacement and colloidal textures in the Mn oxides.

Izvleček

Članek obravnava manganove rude, ki se pojavljajo znotraj visokometamorfnih gnajsov predkambrijske supergrupe Vzhodni Gati na območju Anujurhi v zvezni deželi Odisha, Indija. Zanje so značilne konformne leče, ki vsebujejo minerale, kot so kriptomelan, romanehit, piroluzit, todorokit in pirofanit, skupaj z drugimi neprozornimi minerali, kot so grafit, goethit in ilmenit. Jalovinski minerali v teh rudah vključujejo kremen, glinenec, granat, kaolinit, apatit, silimanit, cirkon, biotit, alunit in gorceiksit. Primarni elementi prisotni v rudi so Si (16,20 %), Mn (15,06 %), Fe (11,94 %) in Al (6,6 %). Dodatno so ugotovili sledne vsebnosti P, K, Ti, Mg, Ca in Na. Povprečno razmerje Fe/Mn, ki znaša 0,81, in diagram primerjave vsebnosti Si z vsebnostmi Al v rudi z območja Anujurhi nakazuje, da feromanganovi sedimenti izvirajo iz mešanih hidrotermalnih virov. Značilnosti manganove rude, kot so odsotnost karbonatnega faciesa rude in geokemična povezava Mn-Ba skupaj z razmerji Na/Mg ter tri komponentnim diagramom CaO-Na_2O-MgO rud jasno kažejo, da gre za metamorfozirano plitvomorsko do jezersko nahajališče. Po odlaganju in diagenezi so manganovi minerali prestali vsaj dve fazi ultra visoke temperature (UHT) in metamorfizma granulitnega faciesa skupaj s prikamnino. Tektonski dvig, erozija, dolga izpostavljenost atmosferskemu kisiku in pronicanju meteorne vode so privedli do supergene spremembe in remobilizacije primarnih manganovih mineralov v koloidnem stanju, čemur je sledila epigenetska zamenjava vzdolž strukturno šibkih površin kamnin granulitnega faciesa, kar je povzročilo nastanek sedanjih ležišč. To dokazujejo opazovane sekundarne zamenjave in koloidne teksture v Mn oksidih.

Introduction

Manganese makes up about 0.1 to 0.2 % of the Earth's crust, ranking as the 10th most abundant element (Post, 1999). It exists in three different oxidation states in natural systems: +2, +3, and +4, leading to a variety of multivalent phases. Manganese oxide minerals have been utilized for many years by ancient civilizations for pigments and to clarify glass. By the mid-nineteenth century, manganese became a crucial component in the steel-making industry, which remains the main consumer of manganese ore. Manganese is the primary component in LMO (Lithium manganese oxide) and NMC (Lithium nickel manganese cobalt) batteries due to its cost-effectiveness compared to other battery metals and its abundant supply (Parrotti et al., 2023). Over 30 manganese oxide/ hydroxide minerals are found in various geological settings (Post, 1999).

The total resources/ reserves of manganese ore in India as of 2015 is 495.87 million tonnes. Odisha tops the total reserves/ resources with a 44 % share, followed by Karnataka at 22 % and Madhya Pradesh at 12 %. During 2018–19, the total production of manganese ore was 2.82 million tonnes with Madhya Pradesh as the leading producer of manganese ore at 33 %, followed by Maharashtra (27 %) and Odisha (16 %). Grade-wise, 68 % of the total production was of lower grade (below 35 % Mn), 21 % of medium grade (35–46 % Mn) and 10 % was of high grade (above 46 % Mn) (Indian Minerals Yearbook 2019).

To fulfill the large supply-demand gap of manganese due to the splurge in demand in the steel industry; the limited availability of high-grade (+44 % Mn) manganese ores coupled with the limitations of the domestic manganese ore, made it obligatory for revision of the threshold value of manganese ores to 10 % Mn in exploration and to exploit low-grade manganese ores. For the development or upgradation of low-grade ores, it is important to characterize or know the nature of the low-grade ores of our country, including the chemistry, mineralogy and correlation that will serve the future industrial development (Manganese Ore: Vision 2020 and beyond, IBM, 2014).

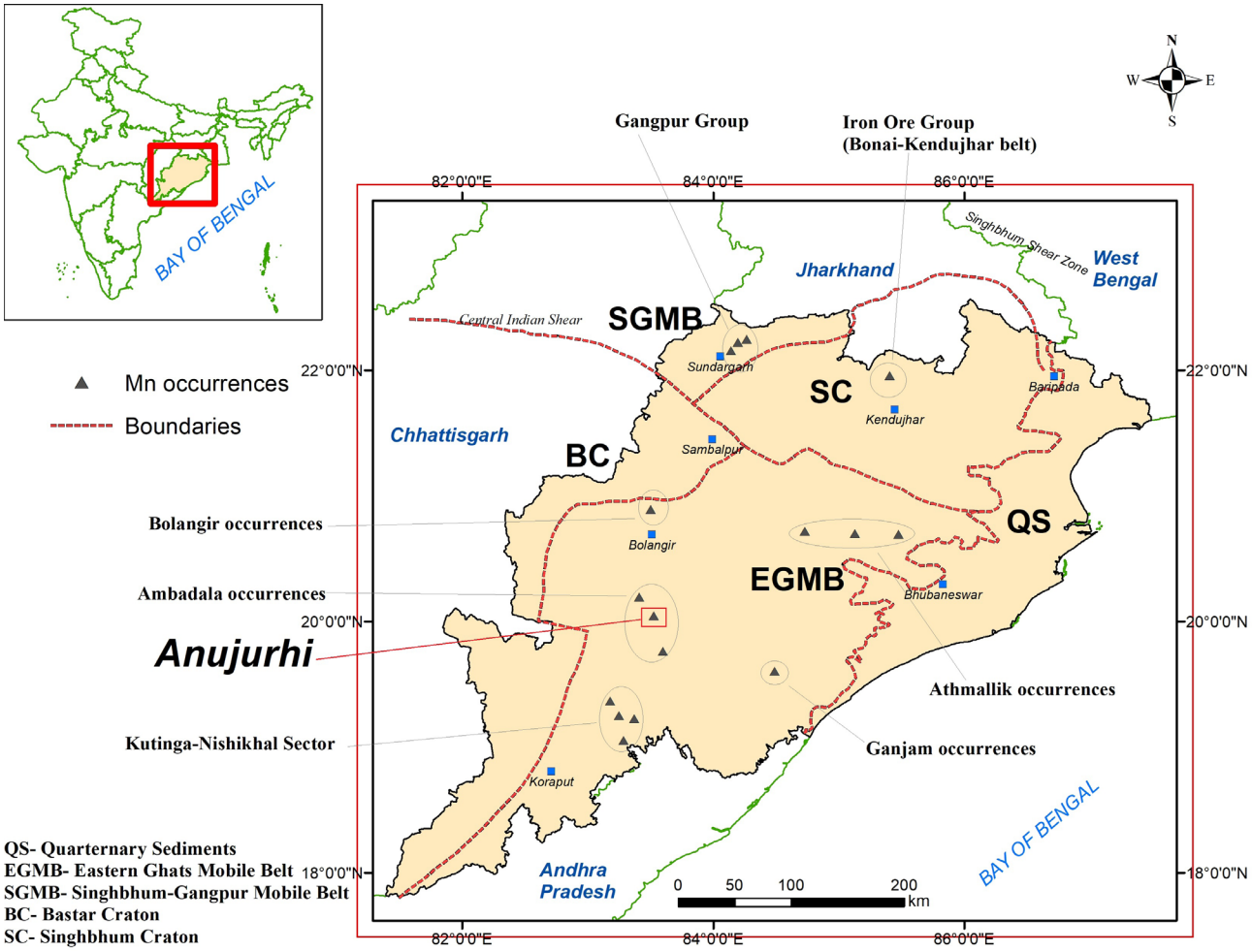

Fig. 1. Map of Odisha state showing the important domains (Cratons, Mobile belts and Quaternary sediment cover) and the known manganese occurrences (Map source- GSI, SU: Odisha).

In the state of Odisha, the manganese ore is found to occur in three stratigraphic horizons and spatially distributed wide apart i.e. Iron Ore Group in Bonai-Keonjhar belt (Roy, 2000), Gangpur Group in Sundergarh district and Eastern Ghats Supergroup in Koraput-Rayagada-Kalahandi-Balangir belt (Roy, 2000; Mishra et al., 2016). The manganese occurrences in the Eastern Ghat Mobile belt have been studied for their economic potential, mineralogical characteristics and evolutional history by several workers like Walker (1902), Dey (1942), Murthy et al. (1971), Narayanswamy (1966, 1975), Acharya et al. (1994, 1997), Ramakrishna et al. (1998), Nanda & Pati (1991), Jena et al. (1995), Rao et al. (2000), Rickers et al. (2001), Dasgupta and Sengupta (2003), Dash et al. (2005), Bhattacharya et al. (2011), Chetty (2014), Karmakar et al. (2009) and others.

The manganese deposits in the Anujurhi-Ambadala-Rukunibori-Loharpadar areas, collectively known as the Ambadala occurrence, confirm the presence of a continuous manganese ore zone spanning 150 km from the Kutinga-Nishikhal sector in the Koraput district of Odisha to the Uchhabapalli-Kanaital sector in the Bolangir district of Odisha (Fig. 1). The explored manganese occurrence is situated approximately 200 m east of Anujurhi village in the Rayagada district of Odisha and falls in Survey of India Toposheet no. 65M/5. This paper will provide an overview of the geology, mineralogy, and geochemistry of the manganese deposits in the Eastern Ghat Supergroup of rocks at Anujurhi, with a focus on characterizing the manganese ores as a potential future economic opportunity. The results obtained will be compared with similar deposits to develop a genetic model that determines the source and formation process of manganese in the Eastern Ghat Mobile Belt.

Geological Setting

The Eastern Ghats Mobile Belt (EGMB) is a Mesoproterozoic collisional orogen (Chetty, 2014), that extends along the east coast of India for over 900 km with a varying width from 50 km in the south to a maximum of 300 km in the north. EGMB or Eastern Ghats Belt (EGB) denotes a contiguous terrain of granulite facies rocks bounded to the north, west and south by the Singhbhum, Bastar and Dharwar Cratons (Dasgupta, 2019), and to the east it disappears underneath alluvial plains and the Bay of Bengal. The EGB consists of an intensely deformed and metamorphosed assemblage of meta-sedimentary and meta-igneous granulite facies rocks, which were subsequently intruded by Proterozoic anorthosite, alkaline rocks and granitoids. The metasedimentary rocks mainly include garnet-sillimanite gneiss (khondalite), quartzites and calc-granulites, while the meta-igneous rocks range from basic to felsic in composition and are essentially hypersthene-bearing charnockites (Chetty, 2014). The protoliths for the Khondalite Group is believed to be dominantly pelitic with subordinate arenaceous and calc- magnesian components (Ramakrishnan et al., 1998; Nanda, 2008) and is indicative of their formation in a shallow water stable shelf milieu (Roy, 2000 & 2006). The minimum age of sedimentation of the Khondalite Group points to an Archean event during 2.8 and 2.6 Ga from the available geochronological data (Roy, 2000).

Ramakrishnan et al. (1998) divided the Eastern Ghats Mobile Belt into four lithotectonic domains longitudinally, viz. Western Charnockite Zone (WCZ), Western Khondalite Zone (WKZ), Central Migmatite Zone (CMZ) and Eastern Khondalite Zone (EKZ). A Transition Zone (TZ) at the contact with the Bastar craton to the west is also marked by a prominent frontal thrust (Dasgupta et al., 2013). Rickers et al. (2001) subdivided EGMB into four crustal domains viz. Domain 1(1A & 1B), Domain 2, Domain 3 and Domain 4, whose boundaries do not match with those of Ramakrishnan et al. (1998) based on Nd-mapping carried out over EGMB. Nd-model ages presented contrasting protolith history in all four crustal domains with domain boundaries marked by prominent shear zones. Later, Dobmeier and Raith (2003) conceptualized EGMB as a collage of four isotopic provinces having distinct geological histories viz. Jeypore, Krishna, Eastern Ghats Province (EGP) and Rengali Province (Fig. 2).

EGB played a dominant role in the configurations of at least three supercontinents Columbia (≈ 1.9-1.4 Ga) (Rogers and Santosh, 2002; Zhao et al., 2002, 2004; Karmakar et al., 2009), Rodinia (≈ 1.0–0.75 Ga) (Li et al., 2008) and Gondwana (≈ 0.55–0.30 Ga). The central domain or EGP (Dobmeier & Raith, 2003) witnessed a prolonged accretion–collision history initiated with rifting and consequent ocean opening and sedimentation at ca. 1.50 Ga during the break-up of Columbia (Upadhyay, 2008; Karmakar et al., 2009) and culminated at ca. 0.90 Ga with the formation of supercontinent Rodinia. The latter united cratonic India with east Antarctica as a separate continent Enderbia that existed until about ca. 0.50 Ga (Karmakar et al., 2009; Dasgupta, 2019).

The metamorphic history of EGP was initiated by a high-T/low-P progressive metamorphism and deformation that eventually led to UHT

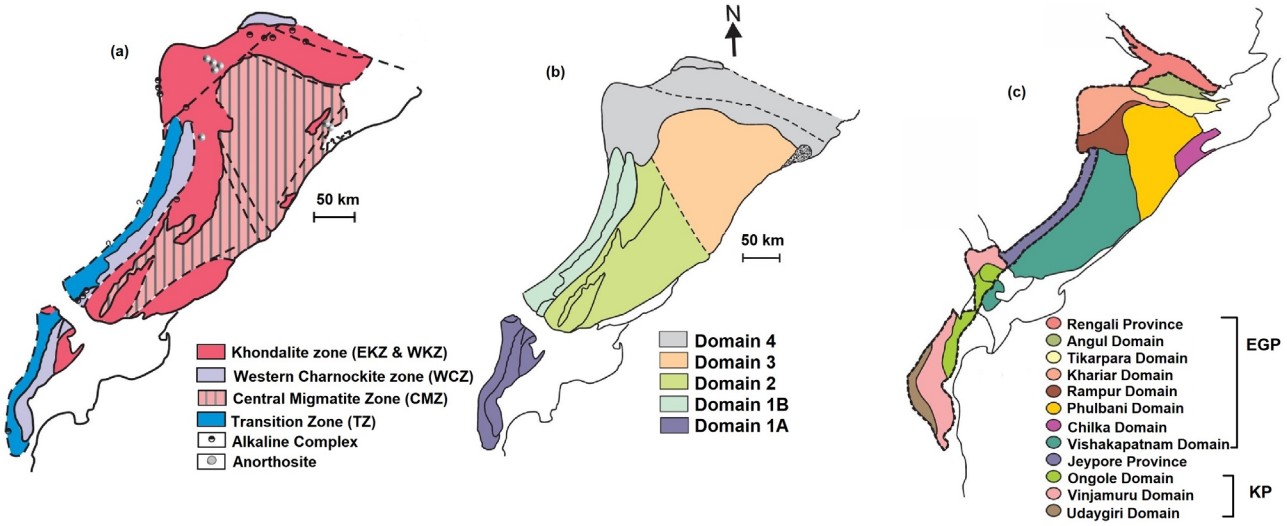

Fig. 2. (a) Geological map of EGB showing lithological divisions by Ramakrishnan et al. (1998), (b) Isotopic domains of EGB of Rickers et al., 2001, (c) Different provinces and domains of EGB by Dobmeier and Raith, 2003 (EGB- Eastern Ghats Belt, EGP- Eastern Ghats Province, KP- Krishna Province).

(~1000 °C) peak (M1-D1) under deep-crustal conditions (8-9 kbar) (Karmakar et al., 2009) ranged from 1.03 Ga (Bose et al., 2011) to 1.13 Ga (Korhonen et al., 2013). A second granulite-grade metamorphism and associated deformation (M2-D2) strongly reworked the deep-crustal granulites and exhumed them to mid-crustal level as evident from decompression-dominated retrogressive segment (Dasgupta & Sengupta, 2003; Dobmeier & Raith, 2003) at 0.95–0.9 Ga with peak conditions of around 7 kbar, 850 °C (Bose et al., 2011; Padmaja et al., 2022). M3 is a weak amphibolite grade overprint and mostly localized along ductile shear zones (Karmakar et al., 2009) constrained at ≈0.55-0.50 Ma (Karmakar et al., 2009). Thermal imprint associated with M3 is manifested by emplacement of pegmatite crosscutting the M2-D2 foliation (Karmakar et al., 2009).

Geology of the Anujurhi area

The area forms a part of the Central Migmatite Zone of Ramakrishnan et al. (1998), Domain 3 of Rickers et al. (2001) and EGP of Dobmeier and Raith (2003). The Khondalite Group comprises a sequence of garnet-sillimanite (± graphite) schists and gneisses (khondalite *senso-stricto*) with relatively minor quartzite and calc-silicate rocks. The manganiferous horizon at Anujurhi is mainly restricted to the contact of quartz-feldspar-garnet-sillimanite gneiss and garnetiferous quartzite.

The manganese mineralization at Anujurhi is both lithologically and structurally controlled and extends for a strike length of about 900 m. The ore zone is continuous with detached outcrops showing varying width ranging from 5 m to 24 m. Five distinct manganese ore lodes were established for the first time at 10 % manganese cut-off in Anujurhi area. The ore bands are narrow, discontinuous and lenticular in shape and parallel to the regional trend of rocks i.e. N20°E–S20°W with moderate dips towards southeast. The area has undergone polyphase deformation with at least three generation viz. F_1 folds are tight to isoclinal folds observed in quartzite/manganiferous quartzite and calc-granulite. The S_1 axial planar cleavage of F_1 folds is parallel to the primary bedding S_0. F_2 folds are mostly open upright mesoscopic folds recorded in calc-granulite and manganiferous quartzite and F_3 folds occur mainly as broad open warps in the khondalites and calc silicates.

Materials and Methods

As a part of the Annual Programme of Geological Survey of India (GSI) during Field Season 2016–2018, the Anujurhi area was investigated for manganese mineralization by way of mapping in detail on 2000 RF in 2 square kilometers to work out the local stratigraphy, structure and disposition of mineralized zones. Subsurface exploration by core drilling was carried out in eleven boreholes to establish the grade, extension and geometry of the ore bodies. Mapping was supported by laboratory studies like whole rock geochemistry, mineral chemistry and petrographic studies of samples from bedrock, pits, trenches and borehole cores. Bedrock samples from *in-situ* manganese ores and manganiferous quartzite were collected with utmost care. Pits and trenches were cut perpendicular to the strike of the ore zone to expose the bedrock and samples were collected by preparing small channels of 50 cm to 1 m in length depending on the width of the zone and mineralogical variation.

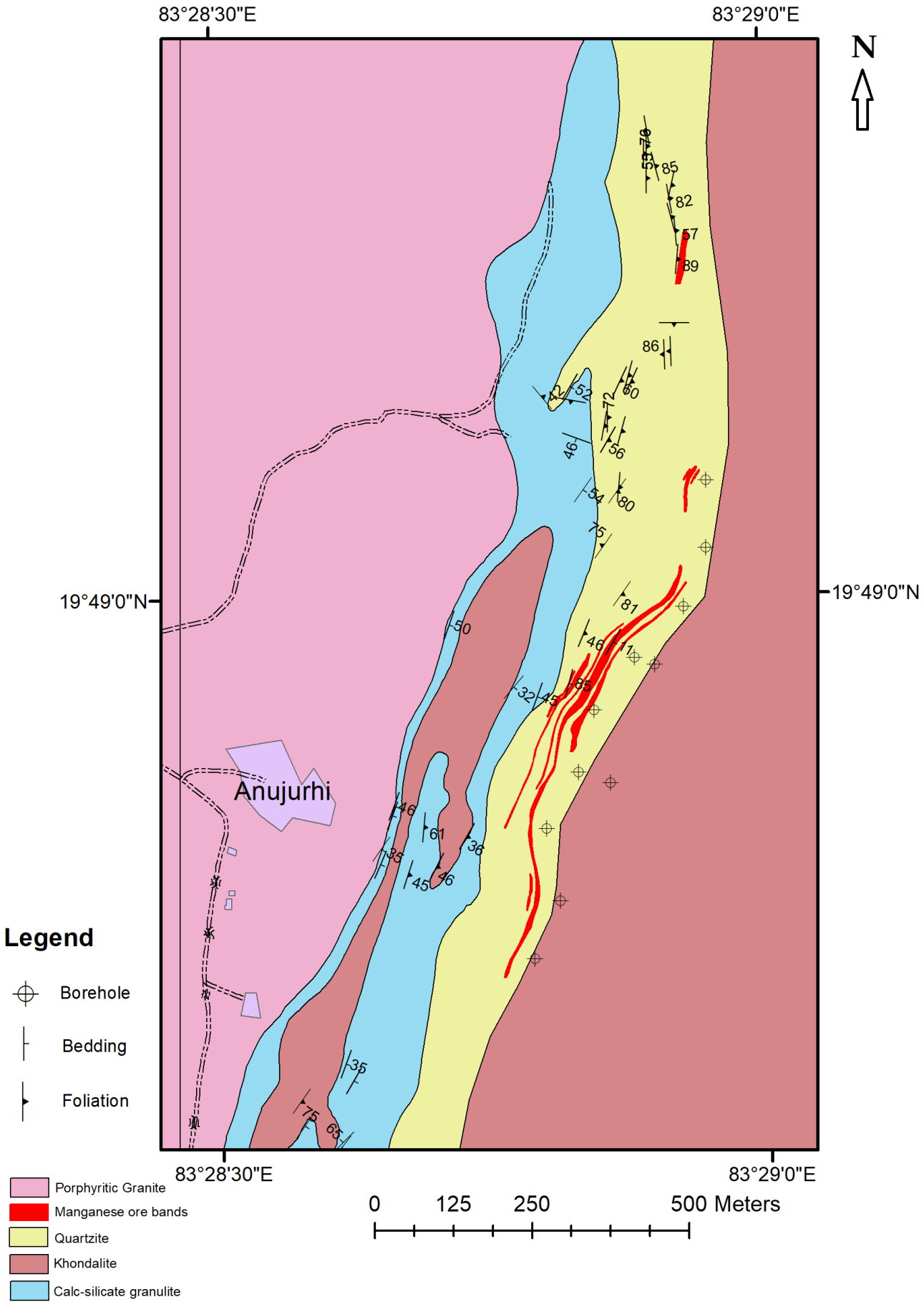

Fig. 3. Geological map of the Anujurhi area showing the manganiferous ore zones.

The core samples of the identified manganiferous zones were collected at a sample interval of 1 m from all the boreholes. Initially, the cores were split into half, half is preserved and the rest is sampled. All the samples collected from bedrock, pit, trench and borehole cores were then powdered manually using mortar and pestle to -120 mesh size. Two sets of samples are prepared by coning and quartering method where one set is submitted for analyses and a duplicate is preserved for future use.

Major element concentrations of 279 whole rock samples were determined through an X-ray fluorescence Spectrometer (Panalytical-ZETIUM) at the Chemical Laboratory, GSI, SU: Odisha by using the pressed pellet technique. The detection limits for this method range from 0.1 % for major and minor elements and 1.0 mg/L for trace elements. Samples from the manganiferous zones were studied under an optical microscope (Leica DM 2500P), the textures exhibited by the manganese ore are of secondary nature mainly replacement and colloform textures.

To confirm the minerals identified in optical microscopy, ten samples from bedrock, trench and cores were analyzed for X-ray diffractometry (XRD), operating at 40 kV and 30 mA with Cu Kα radiation with 1.54 Å wavelength (PANalytical, Model: X'Pert PRO XRD) at Mineral Physics Division, National Centre of Excellence in Geoscience Research, Geological Survey of India, Kolkata. Results are added in Supplementary material (Table 1).

Quantitative chemical analyses of mineral phases have been undertaken at the National Centre of Excellence in Geoscience Research, Geological Survey of India, Kolkata with an automated electron probe microanalyzer (SX 100 CAMECA) with five vertical spectrometers, operating at an acceleration voltage of 15 kV and beam current of 12 nA with beam size of 1 μm. Natural as well as synthetic standards were used during the analyses.

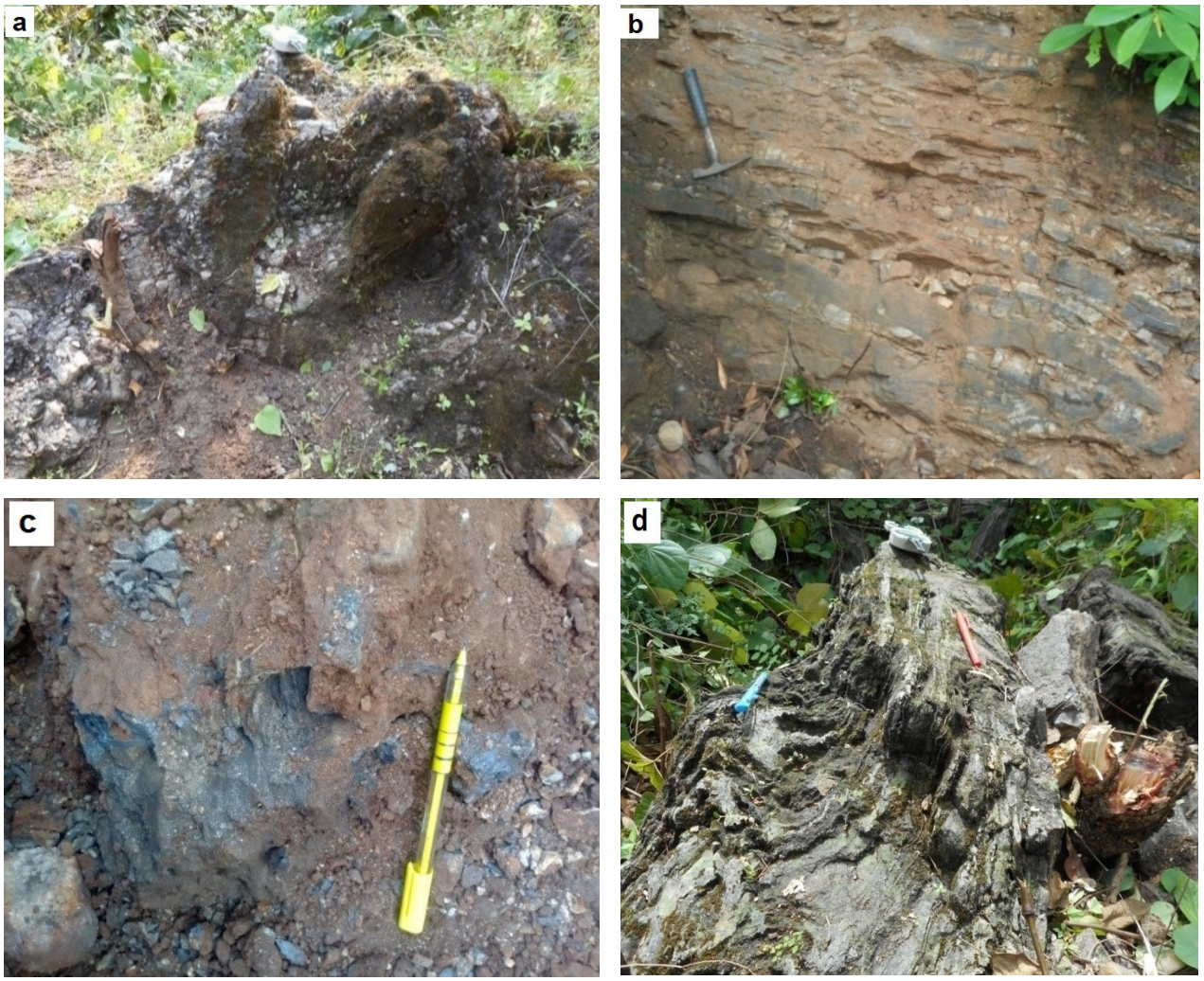

Fig. 4. Disposition of manganese ore zones in Anujurhi area, (a) Folded and silicified manganese ore within quartzite, (b) Fracture filling ore showing parallel bands of manganese ore and silica east of Anujurhi, (c) Soft, friable manganese ore mainly pyrolusite associated with kaolinite east of Anujurhi, (d) Folded manganiferous quartzite.

Results

Field Observations

The ore exhibits a hard, lumpy texture characterized by alternating bands of silica, primarily in the form of recrystallized quartz infilling fractures. In contrast, where associated with clay minerals (e.g. kaolinite) within khondalite, and interfolded with quartzite, the ore becomes soft, friable and powdery. (Fig. 4a, b, c & d).

Ore Petrography

The petrographic analyses revealed a mineral assemblage composed of primary minerals such as quartz (40–50 %), and garnet (10–15 %) respectively followed by Mn-oxides (20–25 %), graphite (5–10 %), goethite (5–10 %), clay minerals (<5 %) and Fe/Mn-Ti oxides (<1 %). The XRD analyses confirm the mineralogy. The chief Mn oxides identified in the area are cryptomelane, romanechite and pyrolusite with minor quantities of todorokite.

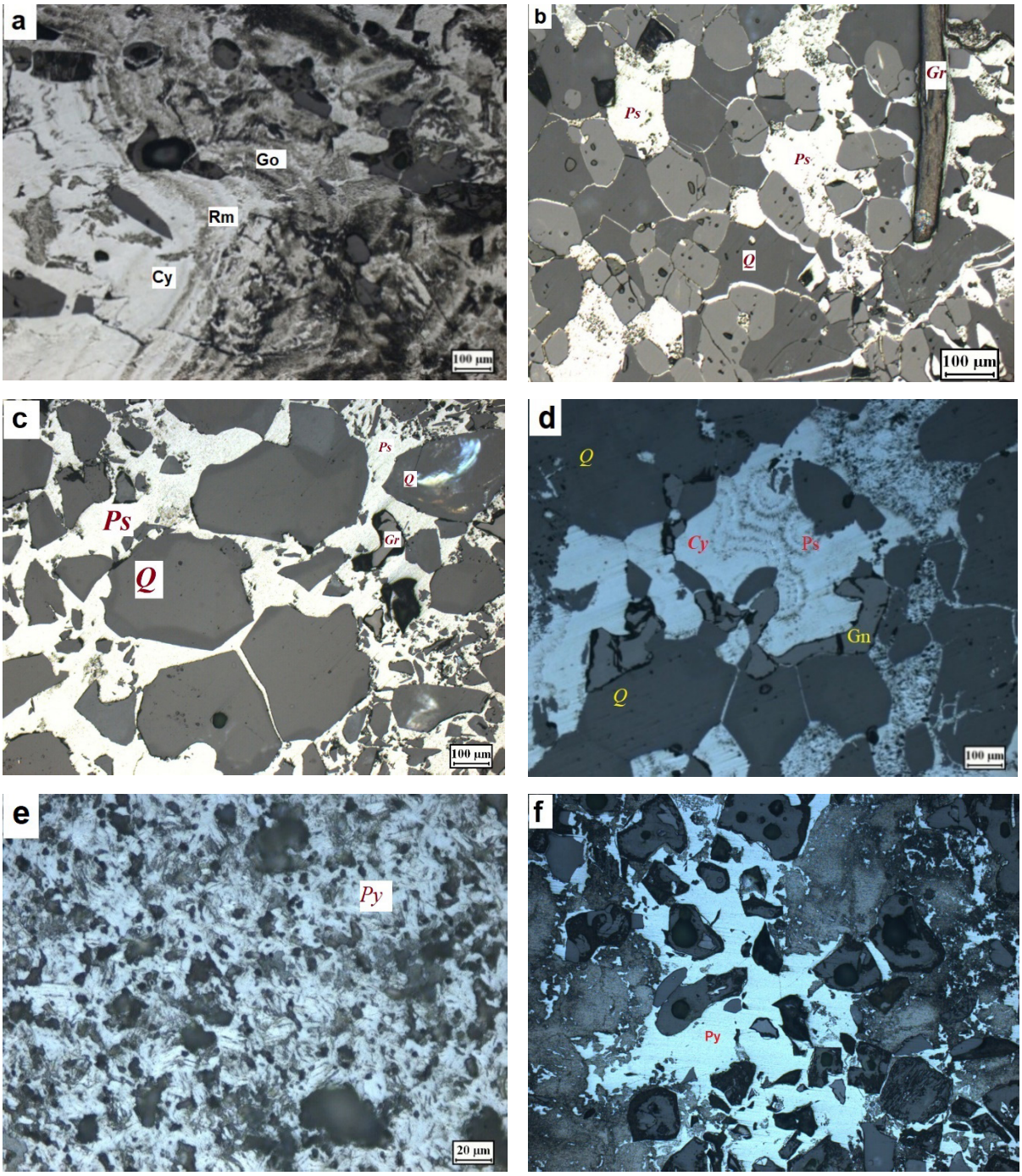

Fig. 5. (a) Colloform bands of cryptomelane (Cy), romanechite (Rm) and goethite (Go), (b) Mosaic grains of quartz & feldspar with fracture filling romanechite (Ps) and flakes of graphite (Gr), (c) Romanechite (Ps) as fracture filling with quartz (Q) and garnet (Gn), (d) Cryptomelane (Cy), Romanechite (Ps) showing colloform banding with quartz (Q) and garnet (Gn) as gangue minerals, (e) Pyrolusite (Py) associated with clay minerals & (f) Pyrolusite (Py) as fracture filling.

The associated gangue minerals are quartz, garnet, graphite, goethite, ilmenite, apatite and zircon, etc.

Since the Mn-oxides share very similar physical and optical characteristics, their identification only with the aid of an optical microscope is difficult, hence, the Mn-oxides were distinguished through EPMA. It is observed that pyrolusite is associated mainly with clay minerals like kaolinite and alunite due to alteration of the quartzo-feldspathic garnet-sillimanite schist or migmatised khondalite. Similarly, a positive correlation is observed between cryptomelane and which is further corroborated by EPMA data. Garnet is generally found as equigranular, mosaic grains associated with quartz and Mn-oxides. The chief ore mineral occupying the intergranular spaces is cryptomelane which forms colloform banding with romanechite and goethite (Fig. 5a, b, c & d). Pyrolusite is mainly confined to the cavity fillings and is often found associated with clay minerals (Fig. 5e & f).

Graphite occurs as scales and flakes within the manganese ores. Goethite is found as gangue showing box work structure, grey with moderate to high reflectivity. Fine crystals of apatite are found embedded in quartz, feldspar and garnet.

Geochemistry

Five representative samples of manganese ore and manganiferous quartzite underwent comprehensive analysis using Electron Probe Microanalysis (EPMA). The results clearly demonstrate that the dominant ore minerals present in the mineralized zones of the Anujurhi area are cryptomelane, romanechite and pyrolusite. Cryptomelane is essentially a potassium-bearing manganese oxide with minor amounts of Ba, Ca, Fe and Al. The K_2O content ranges from 1.93 to 5.24 %. Romanechite occurs together with cryptomelane as a secondary product of alteration of the primary minerals (Fig. 6a & b). BaO content in romanechite is very high which ranges from 16.88 to 18.71 % and Mn content ranges from 46.75 to 49.6 %. Pyrolusite is also present as veins in the host rock, i.e. quartz-feldspar garnet sillimanite schist. Mn content ranges from 60.5 to 61.4 % with minor amounts of Ba, Al and Si. With the EPMA results, the chemical formulae are cryptomlenane–$K_{0.62}(Mn_{7.65},Fe_{0.05},Al_{0.09},Si_{0.02})O_{16}$, romanechite–$(Ba_{0.59},K_{0.01})(Mn_{4.55},Al_{0.04},Si_{0.11})O_{10}$ and pyrolusite-$(Mn_{0.97}Si_{0.01}\ Al_{0.01}Fe_{0.01})O_2$.

The representative EPMA results for cryptomelane & pyrolusite, romanechite, garnet and F-Mn hydroxides are displayed in Table 1 to Table 3.

Garnet is associated with quartz and contains large amounts of Mn (averages of 18.89 %) and Si (averages of 17.47 %). The average Fe and Ca contents were 3.11 wt% and 9.19 wt% respectively. There is an inverse relationship between Mn and (Fe + Ca) results from Mn substitution into spessartines, which have the chemical formulae $[(Mn_{1.9}, Fe_{0.5}, Ca_{0.4})\ Al_2\ (SiO_4)_3]$ and is similar to the spessartine composition of supergene manganese occurrence at Southern Minas Gerais, Brazil (Parrotti, 2023). Two compositional varieties of garnet are reported from the manganese deposits of the Anujurhi area, one variety is rich in spessartine garnet (max. 68 %) whereas the other variety is rich in grossular garnet (max. 46 %) as calculated from the EPMA data. Alteration of the garnet proceeds along the grain boundaries and fractures, often leading to a distinct alteration rim with a

Table 1. Electron microprobe analyses (wt%) of cryptomelane & pyrolusite.

	1	2	3	4	5	6	7	8	9	10	11
SiO_2	0.06	0.1	0.15	0.17	0.1	0.06	0.59	0.15	0.81	0.6	0.69
Al_2O_3	0.31	0.22	0.14	0.24	0.23	0.82	2.68	0.35	0.79	0.86	0.79
MnO	77.84	79.36	78.27	78.4	78.1	75.42	67.39	65.3	78.11	79.32	78.47
MgO	0.07	0.01	0.03	0.01	0.05	0.03	0.04	0.04	0.04	0.06	0.07
Na_2O	0.06	0.17	0.1	0.11	0.07	0.02	0.03	0.13	0.04	0.03	0.02
P_2O_5	0	0	0	0	0	0	0	0	0	0	0
K_2O	4.11	3.98	4.02	4.49	3.9	5.24	4.43	2.3	0.61	0.64	0.59
CaO	0.44	0.49	0.53	0.46	0.45	0.62	0.4	0.48	0.16	0.14	0.19
TiO_2	0	0.02	0	0.02	0	0	0.01	0	0.02	0	0
FeO	0.11	0.11	0.1	0.09	0.2	0.25	3.47	0.02	0.66	0.7	0.53
Cr_2O_3	0	0	0.01	0	0	0	0.1	0	0.31	0.11	0.13
NiO	0	0	0.1	0	0.12	0.14	0.05	0	0.22	0	0.17
BaO	0.29	0.25	0.26	0.21	0.24	0.96	1.5	9.03	1.1	1.04	1.24

Cryptomelane-1 to 8, Pyrolusite-9 to 11

Table 2. Electron microprobe analyses (wt%) of romanechite.

	1	2	3	4	5
SiO_2	0.29	0.64	4.4	0.31	0.47
Al_2O_3	0.46	0.37	0.3	0.51	0.23
MnO	64.06	61.26	61.03	63.85	61.47
MgO	0.05	0.04	0.04	0	0.06
Na_2O	0	0.04	0.04	0.07	0.06
P_2O_5	0	0	0	0	0
K_2O	0.07	0	0.01	0.12	0.15
CaO	0.16	0.25	0.29	0.25	0.38
TiO_2	0	0	0	0	0
FeO	0.13	0.07	0.07	0.19	0.02
Cr_2O_3	0	0	0.2	0.05	0.03
NiO	0.07	0.02	0.01	0	0
BaO	16.88	18.71	17.93	17.2	17.02

central core (Fig. 6c). In rare cases, complete alteration of garnet is also observed. It alters to hydrous oxides/hydroxides of iron and manganese and subsequently cryptomelane (Acharya et al., 1994).

Goethite is a common secondary mineral derived from the alteration of other iron-rich minerals, especially magnetite, pyrite, siderite and hematite under oxidizing conditions. Goethite contains considerable amounts of Al, Si, P and Mn. Phosphorus content is the highest, varying from 0.54 to 2.88 % P_2O_5. Lepidocrocite although less common, has the same origins and they often occur together.

Clay minerals are found in abundance in some sections as a result of deep weathering of host rocks. Gorceixite is a hydrated phosphate ($BaAl_3(PO_4)(PO_3OH)(OH)_6$) that belongs to the alunite group of minerals. It is present as a weathering product of the host rocks like quartz-feldspar-garnet sillimanite schist in the ore zone. In some of the samples, romanechite can be seen altered to gorceixite. P_2O_5 content ranges from 25.43 to 28.76 % and BaO content ranges from 19.1 to 24.47 %. The high amount of phosphorus in samples from Anujurhi can also be attributed to the presence of gorceixite in most samples. Representative EPMA data of gorceixite are given Supplementary material (Table 2).

Pyrophanite in the Eastern Ghats Group of rocks from the Nishikhal area is also reported by Acharya et al. (1994) & in Ambadala area by Pradhan et al. (2016). Pyrophanite is a common accessory mineral associated with metamorphosed manganese-rich rocks. A zoned prismatic grain of ilmenite-pyrophanite is identified in BSE image within cryptomelane with TiO_2 concentration reducing from the center outwards suggesting ilmenite being replaced by Mn-oxides (Fig. 7d). Subhedral prismatic grain of zircons and apatite are rarely found. Representative EPMA data of gorceixite are given in Supplementary material (Table 3).

Table 3. Electron microprobe analyses (wt%) of garnet & Fe-Mn hydroxides.

	1	2	3	4	5	6	7
SiO_2	37.53	37.08	37.61	37.25	2.68	1.17	1.51
Al_2O_3	20.97	20.51	21.31	20.62	2.95	2.1	1.47
MgO	0.22	0.25	0.24	0.9	0.07	0.03	0.03
Na_2O	0.01	0	0.02	0.02	0.09	0.02	0.04
P_2O_5	0	0	0	0	0.54	1.89	2.88
K_2O	0	0.01	0	0	0	0.04	0
CaO	15.99	12.26	18.41	4.8	0.27	0.12	0.04
TiO_2	0.11	0.09	0.03	0.2	0.21	0.07	0.04
FeO	2.63	2.63	1.74	9.03	63.12	68.61	69.97
Cr_2O_3	0.02	0.04	0.03	0	0.07	0.12	0.06
NiO	0	0.02	0	0.1	0.09	0.54	0.22
BaO	0.07	0	0	0.09	0.56	0	0.11
MnO	22.05	27.38	19.45	28.68	7.68	0.9	1.35

Garnet-1 to 4, Fe-Mn hydroxides -5 to 7

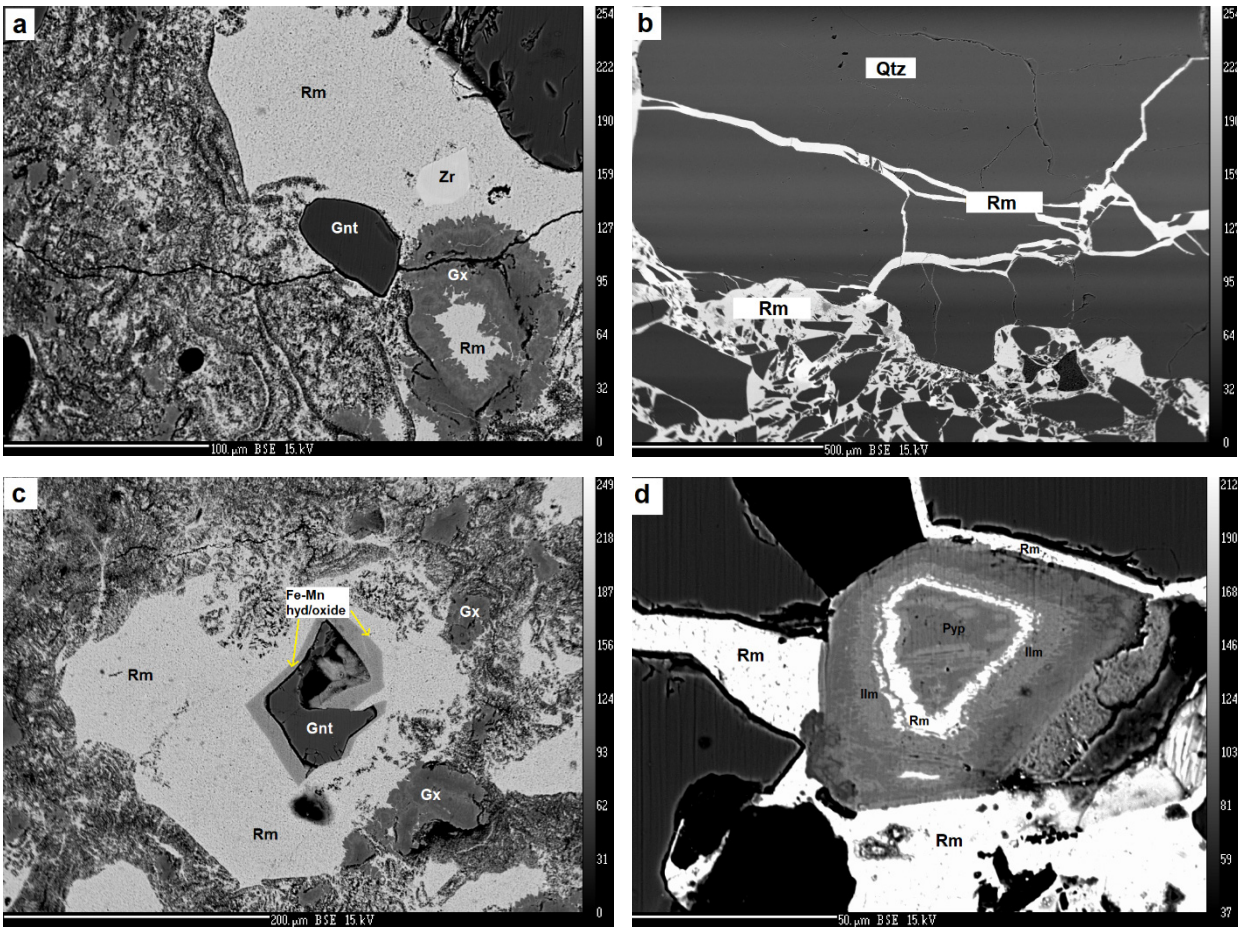

Fig. 6. Back-scattered electron images (EPMA) showing different textures (a) Romanechite (Rm) being altered by clay mineral gorceixite, (b) Romanechite (Rm) as fracture filling in brecciated quartz (qtz), (c) Garnet grains (dark grey) with alteration rims of oxides and/or hydroxides of manganese and iron, enclosed in a matrix of Romanechite (Rm) being altered to Gorceixite (Gx) & (d) ilmenite (Ilm)-pyrophanite (Pyp) zoning within Romanechite (Rm).

Discussion

Diagnostic elemental assemblages of major, minor, and trace metals can be utilized to differentiate manganese deposits formed in various geological environments (Acharya, 1994 & 1997). Such an approach is well established in non-metamorphosed ores (Nicholson, 1992 & 1997) but the application of such diagnostic geochemical signatures to metamorphosed sediments would assume that this signature has been preserved in the meta-sediments of EGB. This argument hinges on the assumption that the original sediment's chemical composition has been retained despite the recrystallization of the mineral assemblage. However, due to the absence of data on minor and trace elements, it was not feasible to accurately define the diagnostic assemblages for different sources of manganese. Upon thorough examination of the chemical data pertaining to the major oxides present in the ores, exhaustive efforts were undertaken to formulate a comprehensive genetic model for the manganese ores located in the Anujurhi area.

The major elements present in the manganese ores of the study area are Si, Mn, Fe and Al, each averaging at 14.82 wt%, 16.60 wt%, 12.42 wt%, and 6.43 wt%, respectively (Table 4). Other elements such as P, K, Ti, Mg, Ca and Na were found to be present in trace amounts (less than 1 wt %). Phosphorous content averaging 0.68 wt % is very high in comparison to other manganese deposits e.g., Noamundi-Koira basin, Odisha (Alvi & Mohd., 2021), Tokoro belt, Japan (Choi & Hariya, 1992) and is a distinguishing property of the manganese ores of EGMB. Phosphorus is either present as definite mineral phases such as apatite, fluor-apatite which is evident from strong positive correlation with Ca (Fig. 7) and gorceixite or in adsorbed state. In adsorbed state phosphorus also occurs within various manganese and associated iron mineral phases like cryptomelane and goethite (Rao et al., 2000). There is enrichment of Na-K-Ca-Mg in Anujurhi manganese ores which is diagnostic assemblage for marine manganese oxides (Nicholson, 1992).

Table 4. Representative chemical composition of manganese ores (wt%).

Sample	ANJ/1	ANJ/2	ANJ/3	ANJ/4	ANJ/5	ANJ/6	ANJ/7	ANJ/8	ANJ/9	ANJ/10
Si	12.53	17.37	16.56	20.35	14.52	15.11	8.69	5.40	17.12	14.91
Al	13.01	13.64	12.04	5.93	5.46	14.31	3.02	5.73	3.95	3.68
Mn	10.94	10.33	11.4	13.58	25.29	10.65	17.06	19.30	12.78	15.37
Fe (T)	8.64	6.35	8.37	11.54	4.03	6.69	27.25	24.54	16.61	18.26
Mg	0.16	0.19	0.20	0.14	0.20	0.14	0.07	0.22	0.02	0.03
Na	0.36	0.27	0.20	0.18	0.17	0.16	0.04	0.04	0.00	0.00
Ti	1.04	0.86	0.72	0.17	0.25	0.84	0.06	0.23	0.22	0.19
Ca	0.69	0.36	0.24	0.24	3.31	0.21	0.10	0.69	0.54	0.64
P	1.41	0.47	0.32	0.29	1.65	0.31	0.68	0.53	0.87	0.60
Mn/Fe	1.27	1.63	1.36	1.18	6.28	1.59	0.63	0.79	0.77	0.84
Si/Al	0.96	1.27	1.38	3.43	2.66	1.06	2.87	0.94	4.33	4.05

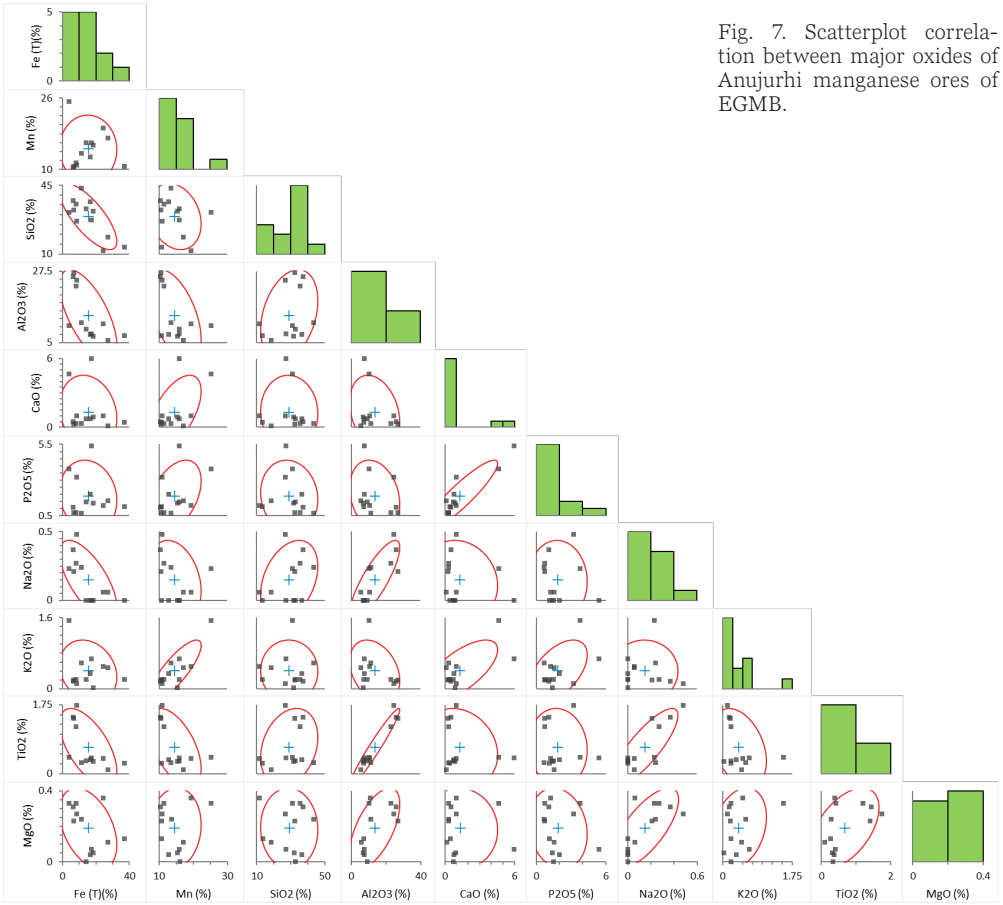

Fig. 7. Scatterplot correlation between major oxides of Anujurhi manganese ores of EGMB.

Genesis of manganese ores

The four sources of material for sedimentary manganese deposits are hydrothermal, hydrogenous, detrital, and diagenetic. Sea-floor hydrothermal crusts typically have fractionated Fe and Mn concentrations, resulting in either Fe-rich (Fe/Mn > 10) or Mn-rich (Fe/Mn < 0.1) deposits. On the other hand, the Fe/Mn ratio of hydrogenous ferromanganese sediments, such as deep-sea manganese nodules, averages about unity (Crerar et al., 1982). The Anujurhi manganese ores have an average Fe/Mn ratio of 0.81, ranging from 0.06 to 3.48, suggesting that the major source is hydrogenous ferromanganese sediments. Hydrogenous deposits are formed by the slow precipitation of Fe and Mn from seawater and are characterized by Mn/Fe ratios between 0.5 to 5 and a relatively high content of trace metals (Bonatti, 1972; Glasby, 1997), similar to that of the Nishikhal manganese ores (Acharya, 1997).

The Si/Al ratio can be used to differentiate between hydrothermal, hydrogenous, and detrital materials and sources (Crerar et al., 1982; Choi and Hariya, 1992). Hydrogenous ferromanganese

nodules typically have a Si/Al ratio of about 3, which is characteristic of marine sediment. Ferromanganese crusts have a mean Si/Al ratio of 5.1, while iron-rich hydrothermal crusts exhibit exceptionally high Si/Al ratios ranging from 600 to 900, suggesting an additional source of Si in these deposits. Some hydrothermal manganese-rich crusts also show high Si/Al ratios, ranging from 10 to 20 (Toth, 1980). The Si/Al ratio in the studied manganese ore ranges from 0.82 to 37.76, with a mean ratio of 3.38 (Fig. 8). Most samples fall within the hydrogenous field, indicating a source from ferromanganese crusts and marine sediments. However, a few samples with high Si/Al ratios fall within the hydrothermal field, suggesting a possible hydrothermal source for some manganese ores. The significant presence of alumina in certain samples can be attributed to the abundant clay minerals resulting from the chemical weathering of host rocks.

The scatter plots of Na against Mg clearly distinguishes manganese oxides deposited in marine, shallow marine and freshwater environments (Nicholson, 1992). The plots of Na *versus* Mg (Fig. 9) lie in the freshwater field of Nicholson (1992) similar to the samples of Nishikhal & Kutinga areas (Acharya, 1994 & 1997). The association of Mn-Ba indicates a probable freshwater origin (Nicholson, 1992). Nonetheless, it's crucial to acknowledge that Ba is also enriched in hydrothermal mineralization (Nicholson, 1992).

The CaO-Na_2O-MgO ternary plot (after Dasgupta et al., 1999) shows that the Mn oxide ores are associated to both marine sedimentary environments and freshwater sedimentation in lakes (Fig. 10). In the Anujurhi area, the prevalence of oxide facies without any manganese carbonate mineral further suggests that the ores were deposited in highly oxidizing environments in shallow water, near shore, or shelf settings (Roy, 1981; Dasgupta et al., 1993; Nicholson et al., 1997). Additionally, the Fe-Si*2-Mn ternary plot after Toth, 1980 also indicates that manganese originated from Fe-Mn crusts and nodules (Fig. 11). Ti is typically not mobile in hydrothermal solutions and is used to gauge the amount of clastic input (Choi & Hariya, 1992). A high concentration of Ti indicates the mixing of detrital material during precipitation, which is backed by a strong correlation between aluminum (Al) and titanium (Ti) as shown in Figure 12.

The khondalite succession consists mainly of shallow-water sediments including orthoquartzite-carbonate suite, arkoses, and semi-pelites, with manganese beds indicating a passive continental margin assemblage (Acharya, 1997; Ramakrishnan et al., 1998; Roy, 2006; Nanda, 2008). In the Anujurhi area, well-defined bands of manganese ore occur with the same strike and dip as the dominant foliation in the quartzite and quartz-feldspar-garnet-sillimanite gneiss. Additionally, the similar imprints of different phases of folds in manganese ore bodies and the country rocks strongly suggest that the manganese ores have developed as a syngenetic part of the metasedimentary sequence of the Eastern Ghats complex.

The sediments, primarily resulting from continental weathering and containing iron and manganese, were transported to deposition sites such as lakes or shallow seas through various mechanisms. These include being carried as finely divided particles in river waters, as adsorbed compounds on clay particles, and as sols and gels. The precipitation of iron and manganese in sedimentary

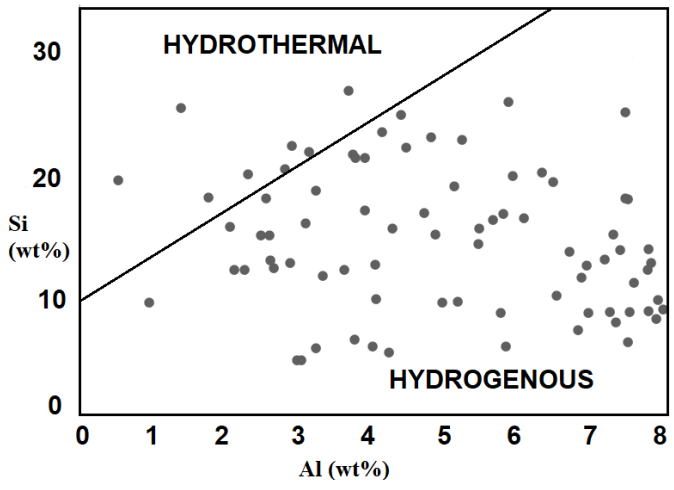

Fig. 8. Plots of Aujurhi manganese ore samples in the Si vs Al graph (Choi & Hariya 1992).

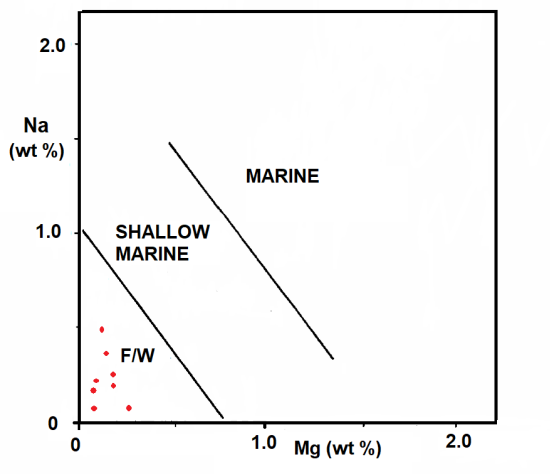

Fig. 9. Na vs Mg discrimination diagram of Nicholson (1992) showing Anujurhi manganese ore samples.

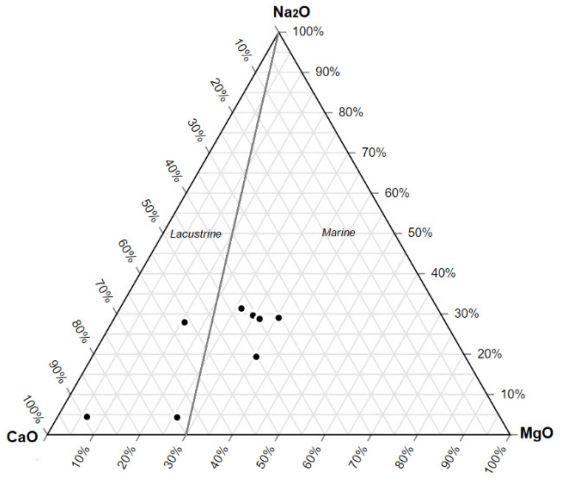

Fig. 10. CaO-Na_2O-MgO ternary plot after Dasgupta et al., 1999 shows majority samples falling in marine field for the manganese ore samples of Anujurhi, EGMB, Odisha.

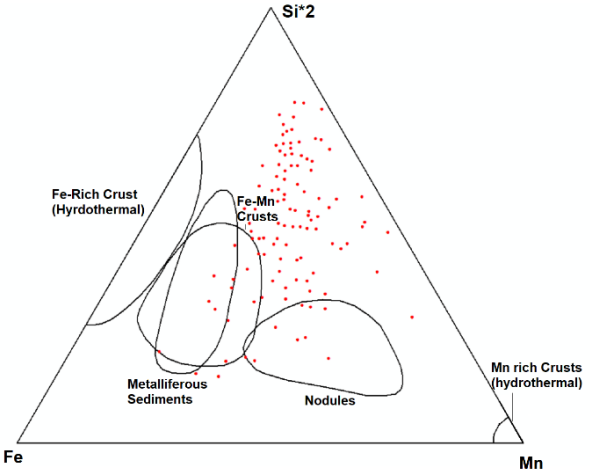

Fig. 11. Fe-Si^x2-Mn ternary plot after Toth, 1980 showing the manganese ore samples showing affiliation towards Fe-Mn crusts and nodules.

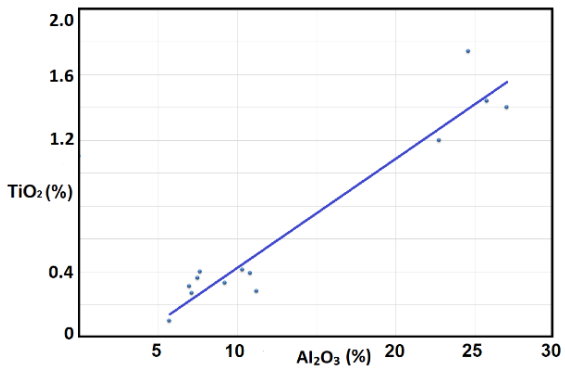

Fig. 12. TiO_2-AI_2O_3 diagram showing positive correlation for the Anujurhi samples.

environments is significantly influenced by Eh-pH conditions. Manganese is soluble at low Eh and precipitates with increasing Eh (under strongly oxidizing conditions) at a pH ranging from 5–8, which corresponds to the pH of surface water to seawater (Maynard, 1983; Nicholson et al., 1997). Iron and manganese may have precipitated as iron and manganese hydroxides and oxides (Mn^{4+}) in the presence of free oxygen. During early diagenesis, Mn^{4+} oxides are reduced to Mn^{2+} oxides through anaerobic reduction.

The model is supported by geochronological data indicating that the protolith ages of the meta-sedimentary rocks of Domain 3 in Eastern Ghats are approximately ≈ 2.2 Ga to 1.8 Ga (Rickers et al., 2001). This coincides with the worldwide first major deposition of sedimentary manganese during the early Paleoproterozoic era, lasting until 1.8 Ga, which occurred concurrently with the Great Oxygenation Event (GOE) between 2.45 Ga to 2.1 Ga (Spinks, 2018). These manganese ores have undergone multiple phases of deformation along with the host rocks, as evidenced by the folding of manganese ore bands and their parallel disposition to the S_2 foliation.

The manganese formations and associated host rocks have experienced at least two phases of ultra-high temperature (UHT) metamorphism at around 1100 Ma and granulite facies metamorphism at approximately 950-900 Ma, which are related to the breakup of the Supercontinent Columbia and the assembly of the Supercontinent Rodinia (Karmakar et al., 2009; Bose et al., 201; Dasgupta, 2019). With an increase in pressure and temperature during metamorphism, the manganese minerals of higher valency states were transformed into oxides of relatively lower valency (Roy, 1981; Acharya, 1997).

After the post-metamorphic period around 950-900 Ma, the Eastern Ghats and Rayner Complex amalgamated during the formation of the Supercontinent Rodinia (Karmakar et al., 2009). This caused tectonic uplift and prolonged exposure to atmospheric oxygen and percolation of meteoric water, leading to the alteration of primary minerals through supergene enrichment. The primary manganese oxide minerals were largely obliterated, evident from the absence of primary manganese oxides and alteration of Mn- silicate like spessartine. Under these supergene conditions, the strong oxidation effects caused a transformation of the lower valency manganese oxides (primary minerals) into higher valency oxides such as cryptomelane, romanechite, and pyrolusite (Acharya et al., 1994). An intriguing example of this transformation is the development of romanechite and/or cryptomelane and goethite from the manganese garnet (spessartine) i.e. supported by petrography and EPMA. The mineral-rich fluid may have journeyed through surface run-off or meteoric water to structurally weak planes like shear and fracture planes of the meta-sedimentaries, where Mn and

Fe reprecipitated as cavity filling and replacement deposits, predominantly containing quartz and feldspar. The replacement and colloidal textures of the secondary manganese oxides provide compelling evidence for this origin.

The remobilized supergene manganese ores occur as lensoidal ore bodies within the granulite facies of rocks of EGB, persisting for a significant strike length. These ore bodies have been confirmed to exist up to a depth of 30–35 m from the surface through drilling. The manganese content in these EGB ores, averaging around 15 %, is lower than that of the Iron Ore Group (Mohapatra et al., 2009) and can be classified as ferruginous manganese ore. The high phosphorus content in these ores presents a challenge for commercial recovery, as evidenced in the case of Kutinga-Nishikhal ores (Acharya et al., 1994 & 1997; Rao et al., 2000). However, characterizing these low-grade ores for their mineralogy and association could unlock promising prospects for future utilization. Hence, a thorough study of these ores in the future could be undertaken using Raman Spectroscopy in conjunction with Scanning Electron Microscope (SEM) studies, accompanied by trace element geochemistry analysis. This approach is expected to provide detailed insights into the mineralogy and geochemical behavior of the processes involved during the supergene enrichment and subsequent mobilization to form commercially viable deposits.

Acknowledgements

The authors would like to express their gratitude to the Deputy Director General of the Geological Survey of India, State Unit: Odisha, for providing administrative and financial support to this work between 2016 and 2018. The study was conducted as part of the mineral exploration project (FSPID: ME/ER/ODS/2016/008 & M2AFGBM-MEP/NC/ER/SU-ODS/2017/12919). The authors are also thankful to Shri Bijay Kumar Sahu, Retired Deputy Director General, GSI, and Shri Manoj Kumar Patel, Retired Deputy Director General, GSI, for their suggestions, guidance, and supervision during fieldwork. The authors express their appreciation to the personnel working in Petrological Lab of Odisha, the Chemical Lab of Eastern Region, Mineral Physics Division and EPMA lab of NCEGR at Central Headquarters, GSI, Kolkata, for their timely submission of results and cooperation during lab work.

Conflict of interest

The authors certify that there is no conflict of interest with any individual or any organization.

References

Acharya, B.C., Rao, D.S. & Sahoo, R.K. 1997: Mineralogy, geochemistry and genesis of Nishikhal manganese ore deposit, South Orissa, India. Min. Deposita, 32, 79–93. https://doi.org/10.1007/s001260050074

Acharya, B.C., Rao, D.S & Sahoo, R.K. 1994: Mineralogy and genesis of Kutinga manganese deposit, South Orissa, India. J. Min. Petr. Econ. Geol. 89: 317–328. https://doi.org/10.2465/ganko.89.317

Alvi, S.H. & Shaif Mohd. 2021: Geochemical signatures of manganese ores around Barbil, Noamundi-Koira basin, Singhbhum Craton, Eastern India. Geology, Ecology, and Landscapes, 5/4: 260–268. https://doi.org/10.1080/24749508.2020.1720489

Bhattacharya, S., Kar, S., Saw, A.K., Das & P. 2011: Relative Chronology in High-Grade Crystalline Terrain of the Eastern Ghats, India: New Insights. Int. Jour. Geosciences, 2: 398–405

Bhattacharya, A. & Gupta, S. 2001: A reappraisal of polymetamorphism in the Eastern Ghats belt – A view from north of the Godavari rift. Proc. Indian Acad. Sci, 110/4: 369–383. https://doi.org/10.1007/BF02702901

Bose, S., Dunkley, D.J., Dasgupta, S., Das, K. & Arima, M. 2011: India–Antarctica– Australia–Laurentia connection in the Paleo Mesoproterozoic revisited: evidence from new zircon U–Pb and monazite chemical age data from the Eastern Ghats Belt, India. Geol. Soc. of America Bulletin, 123: 2031–2049.

Chetty, T.R.K. 2014: Deep crustal Shear Zones in the Eastern Ghats Mobile Belt, India: Gondwana correlations. J. Ind. Geophysics. Union, 18, 19–56

Choi, J.H. & Hariya, Y. 1992: Geochemistry and depositional environment of manganese oxide deposits in Tokoro belt, northeastern Hokkaido, Japan. Econ. Geol. 87/5: 1265–1274. https://doi.org/10.2113/gsecongeo.87.5.1265

Crerar, D.A., Namson, J., Chyi, M.S., Williams, L. & Feigenson, M.D. 1982: Manganiferous Cherts of the Franciscan Assemblage: I. General Geology, Ancient and Modern Analogues, and Implications for Hydrothermal Convection at Oceanic Spreading Centers. Economic Geology, 77/3: 519–540. https://doi.org/10.2113/gsecongeo.77.3.519

Dash, C., Behera, S.N. & Patel, S.N. 2009: Delineation of potential Manganese ore bands/bodies within the Manganiferous horizon of the central sector of the Eastern Ghats Granulite Belt in Orissa covering parts of Bolangir, Kalahan-

di and Rayagada districts (P-II). Unpublised G.S.I report (2003-2005).

Dash, C. & Behera, S.N. 2009: Search for potential manganese ore bands/bodies within the manganiferous horizon of the eastern part of the Eastern Ghats granulite belt in Orissa covering parts of Angul and Boudh district s, (P - I). Unpublised G.S.I report.

Dasgupta, H.C., Sambasiva Rao, V.V. & Krishna, C. 1999: Geology, geochemistry and genesis of the freshwater, precambrian manganese deposit of the iron ore group from Noamundi basin, Eastern India. Indian J. Geol., 71: 247–264

Dasgupta, S. & Sengupta, P. 2003: Indo-Antarctic correlation: a perspective from the Eastern Ghats Granulite Belt, India. In: Yoshida, M., Windley, B.F. & Dasgupta, S. (eds.): Proterozoic East Gondwana: Supercontinent Assembly and Breakup. Geological Society, London, Special Publications, 206: 131–143.

Dasgupta, S. 2019: Petrological evolution of the Eastern Ghats Belt- Current status and future directions. IUGS, 43/1: 124–131. https://doi.org/10.18814/epiiugs/2020/020007

Dasgupta. S., Bose, S. & Das, K. 2013: Tectonic evolution of the Eastern Ghats Belt, India. Prec. Res., 227: 247–258. https://doi.org/10.1016/j.precamres.2012.04.005

Dobmeier, C.J. & Raith, M.M. 2013: Crustal architecture and evolution of the Eastern Ghats Belt and adjacent regions of India, Geol. Soc. Spec. Publ., 206: 145–168. https://doi.org/10.1144/GSL.SP.2003.206.01.09

Glasby, G.P. 1977: Marine manganese deposits. Elsevier Oceanography Series, 15. New Zealand: 45–52.

Jena, S.K., Devdas, V. & Bhattacharya, S.K. 2001: Final report on the exploration for manganese ore in Kutinga block and adjoining areas of Koraput, Rayagada and Bolangir districts, Orissa. Unpublished G.S.I report

Karmakar, S., Bose, S. & Dasgupta, S. 2009: Proterozoic Eastern Ghats Belt, India – a witness of multiple orogenies and its lineage with ancient supercontinents. Journal of the Virtual Explorer, Electronic Edition, 32, paper 3.

Korhonen, F.J., Clarke, C., Brown, M., Bhattacharya, S. & Taylor, R. 2013: How long-lived is ultrahigh temperature (UHT) metamorphism? Constraints from zircon and monazite geochronology in the Eastern Ghats orogenic belt, India. Prec. Res. 234: 322–350. https://doi.org/10.1016/j.precamres.2012.12.001

Li, Z.X., Bogdanova, S.V., Collins, A.S., Davidson, A., De Waele, B., Ernst, R.E., Fitzsimons, I.C.W., Fuck, R.A., Gladkochub, D.P., Jacobs, J., Karlstrom, K.E., Lu, S., Natapov, L.M., Pease, V., Pisarevsky, S.A., Thrane, K. & Vernikovsky, V. 2008: Assembly, configuration, and break-up history of Rodinia: A synthesis. Prec. Res., 160: 179–210. https://doi.org/10.1016/j.precamres.2007.04.021

Manganese Ore: Vision 2020 and Beyond 2014: Indian Bureau of Mines, Govt. of India, Ministry of Mines.

Maynard, J.B. 1983: Geochemistry of Sedimentary Ore Deposits. Springer-Verlag New York Inc.: 121–145

Nanda, J.K. 2008: Tectonic Framework of Eastern Ghats Mobile Belt. An Overview. Memoir Geological Society of India, 74: 63—87.

Nicholson, K. 1992: Contrasting mineralogical-geochemical signatures of manganese oxides: Guides to metallogenesis. Economic Geology, 87/5: 1253–1264.

Nicholson, K., Hein, J.R., Buhn, B. & Dasgupta, S. 1997: Manganese Mineralization: Geochemistry and Mineralogy of Terrestrial and Marine Deposits. The Geological Society Special Publication, 119.

Padmaja, J., Sarkar, T., Sorcar, N., Mukherjee, S., Das, N. & Dasgupta S. 2022: Petrochronological evolution of Mg-Al granulites and associated metapelites from the contact zone of the Archean Bastar Craton and Proterozoic Eastern Ghats Province, and its implications. Geosystems and Geoenvironment, 1/4: 100041. https://doi.org/10.1016/j.geogeo.2022.100041

Parrotti, D.D., da Conceição, F.T. & Navarro, G.R.B. 2023: The Mineralogy, Geochemistry and Origin of the Supergene Manganese Occurrences in the Southern Minas Gerais, Brazil. Minerals, 13/9: 1216. https://doi.org/10.3390/min13091216

Post, J.E. 1999: Manganese oxide minerals: Crystal structures and economic and environmental significance. Proc. Natl. Acad. Sci. USA, 96/7: 3447–3454. https://doi.org/10.1073/pnas.96.7.3447

Pradhan, S., Mishra, P.P., Dash, N., Mishra, P.C., Khaoash, S. & Mohapatra, B.K. 2016: Manganese mineralization in parts of Eastern Ghats around Ambadola, Rayagada District, Odisha. Vistas in Geological Research, Special Publication in Geology, 14: 42–48.

Ramakrishnan, M., Nanda, J.K. & Augustine, P.F. 1998: Geological evolution of the Proterozoic Eastern Ghats mobile belt. Proc. Workshop on Eastern Ghats Mobile Belt, Geol. Surv. Ind., Spec. Publ: 44.

Rao, D.S., Acharya, B.C., Sahoo & R.K. 2000: Role of mineralogy, mineral chemistry and geochemistry in mineral processing: A case study for high phosphorus manganese ores of Nishikhal, South Orissa, India. Processing of Fines, 2: 25–40.

Rickers, K., Mezger, K. & Raith, M.M. 2001a: Evolution of the continental crust in the proterozoic Eastern Ghats belt, India and new constraints for rodinia reconstruction: implications from Sm-Nd, Rb-Sr and Pb-Pb isotopes. Prec. Res. 112: 183–210.

Rogers, J.J.W. & Santosh, M. 2002: Configuration of Columbia, a Mesoproterozoic supercontinent. Gond. Res., 5: 5–22.

Roy, S. 1981: Manganese Deposits. Academic Press, London.

Roy, S. 2000: Late Archean initiation of manganese metallogenesis: its significance and environmental controls. Ore Geol. Rev., 17: 179–198.

Roy, S. 2006: Sedimentary manganese metallogenesis in response to the evolution of the Earth system. Earth-Science Reviews, 77: 273–305.

Spinks, S.C., Thorne, R.L., Sperling, E., White, A., Armstrong, J., leGras, M., Birchall, R. & Munday, T. 2018: Sedimentary Manganese as Precursors to the Supergene Manganese Deposits of the Collier Group; Capricorn Orogen, Western Australia. CSIRO, Australia. EP18235. 36.

Toth, J.R. 1980: Deposition of submarine crusts rich in manganese and iron. Geological Society of America Bulletin, Part I, V. 91: 44–57. https://doi.org/10.1130/0016-7606(1980)91%3C44:-DOSCRI%3E2.0.CO;2

Upadhyay, D. 2008: Alkaline magmatism along the southeastern margin of the Indian shield: implications for regional geodynamics and constraints on craton-Eastern Ghats Belt suturing. Prec. Res. 162: 59–69. https://doi.org/10.1016/j.precamres.2007.07.012

Walker, T.L. 1902: Geology of Kalahandi State, Central Provinces. Memoir, Geological Survey of India, 33: 1–22.

Zhao, G., Cawood, P.A., Wilde, S.A. & Sun, M. 2002: Review of global 2.1-1.8 Ga orogens: implications for a pre Rodinia supercontinent. Earth Sci. Rev., 59/1–4: 125–162. https://doi.org/10.1016/S0012-8252(02)00073-9

Zhao, G., Sun, M, Wilde, S.A. & Li, S. 2004: A Paleo Mesoproterozoic supercontinent: assembly, growth and breakup. Earth Sci. Rev., 67: 91–123. https://doi.org/10.1016/j.earscirev.2004.02.003